View metadata, citation and similar papers at core.ac.uk
brought to you by CORE
provided by Elsevier - Publisher Connector

Current Biology, Vol. 12, 2111–2117, December 23, 2002, ©2002 Elsevier Science Ltd. All rights reserved. PII S0960-9822(02)01390-8

The Large GTPase Dynamin Associates with the Spindle Midzone and Is Required for Cytokinesis

Heather M. Thompson,[1,6] Ahna R. Skop,[2,4,6] Ursula Euteneuer,[3] Barbara J. Meyer,[2,4] and Mark A. McNiven[1,5]

[1]GI Basic Research and Department of Biochemistry and Molecular Biology
Mayo Clinic and Mayo Graduate School
Rochester, Minnesota 55905
[2]Department of Molecular and Cell Biology
University of California, Berkeley
Berkeley, California 94720
[3]ABI Cell Biology
University of Munich
Munich 80336
Germany
[4]Howard Hughes Medical Institute
University of California, Berkeley
Berkeley, California 94720

Summary

Cytokinesis involves the concerted efforts of the microtubule and actin cytoskeletons as well as vesicle trafficking and membrane remodeling to form the cleavage furrow and complete daughter cell separation (for reviews, see [1–6]). The exact mechanisms that support membrane remodeling during cytokinesis remain largely undefined. In this study, we report that the large GTPase dynamin, a protein involved in membrane tubulation and vesiculation [7, 8], is essential for successful cytokinesis. Using biochemical and morphological methods, we demonstrate that dynamin localizes to the spindle midzone and the subsequent intercellular bridge in mammalian cells and is also enriched in spindle midbody extracts. In *Caenorhabditis elegans*, dynamin localized to newly formed cleavage furrow membranes and accumulated at the midbody of dividing embryos in a manner similar to dynamin localization in mammalian cells. Further, dynamin function appears necessary for cytokinesis, as *C. elegans* embryos from a *dyn-1 ts* strain [9], as well as dynamin RNAi-treated embryos, showed a marked defect in the late stages of cytokinesis. These findings indicate that, during mitosis, conventional dynamin is recruited to the spindle midzone and the subsequent intercellular bridge, where it plays an essential role in the final separation of dividing cells.

Results and Discussion

Dynamin Is a Component of the Mitotic Spindle, the Spindle Midzone, and the Intercellular Bridge during Mitosis

The insertion of membrane at the cleavage furrow is an important component of cytokinesis, as it appears that membrane donated from the cell surface alone is not sufficient to support cleavage furrow ingression and separation of daughter cells. Recent work in a variety of systems suggests that proteins involved in vesicle trafficking, such as members of the rab family of GTPases, vesicle coat proteins, and syntaxins, contribute to the completion of cytokinesis (for reviews, see [4–6]). In addition, the delivery and insertion of new membrane at the furrow has been demonstrated to be a late, separate event of cytokinesis [10, 11]. Since dynamin is a component of the vesicular trafficking machinery, we tested whether dynamin functions in cytokinesis by first determining if dynamin is a component of the mitotic spindle or cleavage furrow in dividing epithelial cells. We used indirect immunofluorescence confocal microscopy to analyze the distribution of dynamin during mitosis in Clone 9 cells, a normal rat liver cell line. Interestingly, dynamin was detected as punctate spots surrounding the two microtubule-organizing centers as they began to separate during early prophase as well as around the disassembling nuclear membrane (Figures 1A and 1A′). As the cells progressed through mitosis, dynamin was detected both in the cytoplasm as well as along the mitotic spindle during metaphase (Figures 1B and 1B′), and it then translocated to the spindle midzone region during early anaphase (Figures 1C and 1C′). During late anaphase/early telophase, dynamin colocalized with microtubules of the spindle midzone proximal to the cleavage plane (Figures 1D and 1D′). Finally, in late telophase, during the final stages of cytokinesis, dynamin accumulated at the intercellular bridge near the protein-dense midbody (Figures 1E and 1E′). Interestingly, dynamin was not detected along the entire bundle of intercellular bridge microtubules but was instead detected in regions near the midbody where the final separation event would presumably occur.

To further confirm the intense and interesting dynamin staining at the intercellular bridge during cytokinesis, we tested whether a second pan-dynamin antibody made to a distinct peptide, MC-64, could also detect dynamin at this structure. Indeed, similar dynamin staining of the intercellular bridge was also observed with this second antibody (Figure 2A). As an additional control, Clone 9 cells were stained with preimmune serum, which did not stain the intercellular bridge (data not shown). Next, we tested whether dynamin localized to all microtubule bundles or specifically to the microtubule bundles comprising the intercellular bridge. To this end, Clone 9 cells were treated with Taxol to induce large microtubule bundles and were then fixed and processed as before. In Taxol-treated cells, dynamin was not detected along microtubule bundles (Figures 2B and 2B′) to the extent that it was detected at the intercellular bridge proximal to the midbody (Figures 2C and 2C′). Thus, dynamin appears to be a specific component of the intercellular bridge and not microtubule bundles in general.

To provide higher resolution images of the dynamin-midbody interaction, immunoelectron microscopy was used. For these studies, partially synchronized human (HeLa) or mouse (L929) cells were fixed, embedded,

[5]Correspondence: mmcniven@mayo.edu
[6]These authors contributed equally to this work.

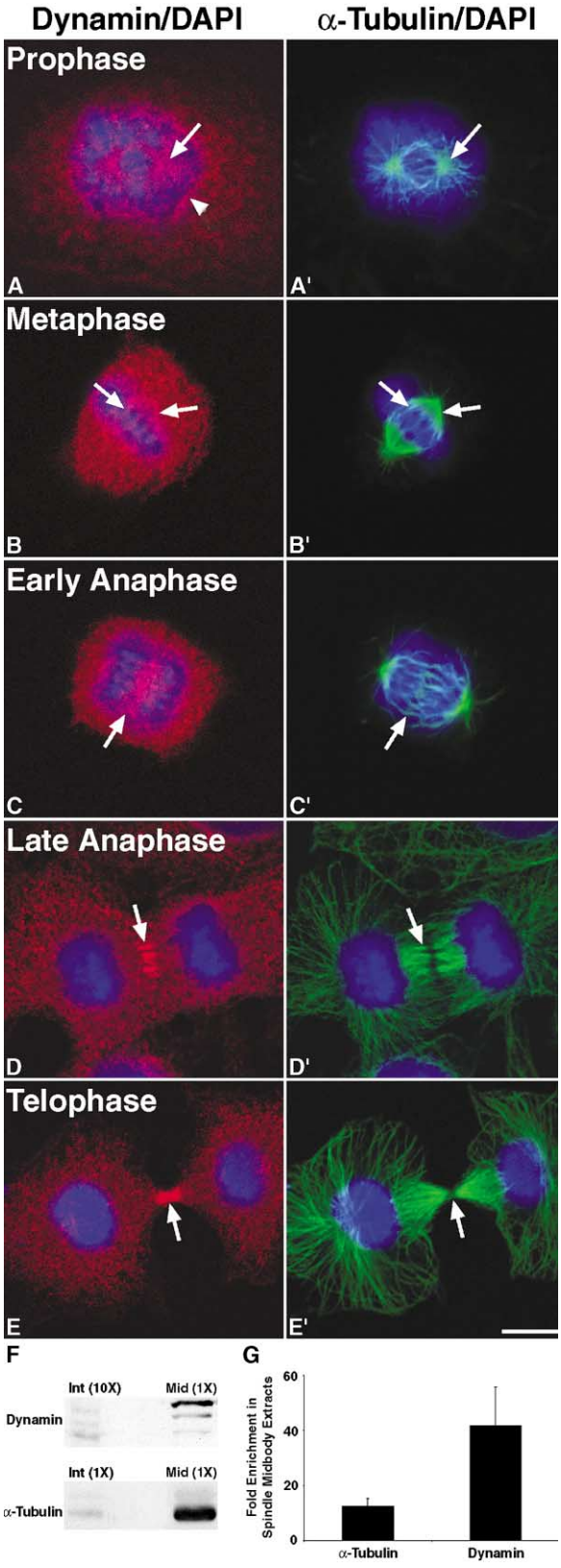

Figure 1. Dynamin Associates with the Mitotic Spindle, Midzone Microtubules, and Intercellular Bridge during Mitosis and Is Enriched in CHO Cell Spindle Midbody Extracts

Cultured Clone 9 cells, a rat hepatocyte cell line, were fixed in −20°C methanol or 3% paraformaldehyde, triple labeled for dynamin (MC-63, red) [33], microtubules (α-Tubulin, green), and DNA (DAPI, blue), then viewed as 1 μm sections with a Zeiss Axiovert 35 confocal microscope.

(A and A′) During early prophase, (A) dynamin was mostly observed in the cytoplasm; however, a population of dynamin was detected around the ([A] and [A′], arrow) separating centrosomes as well as on what appeared to be the (A, arrowhead) nuclear membrane.

(B and B′) Even though the dynamin staining was still mostly cytoplasmic in metaphase cells, a distinct labeling of the ([B′], arrows; two regions of the mitotic spindle are indicated) mitotic spindle was also noted in the ([B], arrows) dynamin channel.

(C–D′) As the cells progressed to (C and C′) early and then (D and D′) late anaphase, the (C and D) dynamin staining became more enhanced at the ([C] and [C′], arrow) spindle midzone and ([D] and [D′], arrow) colocalized with midzone microtubules near the plane of cleavage.

(E and E′) Finally, during late telophase, the majority of the (E) dynamin staining was detected along the (E′) intercellular bridge as two intense bands on each side of the ([E] and [E′], arrow) midbody. The scale bar represents 10 μm.

(F and G) CHO cell extracts from Taxol-treated cells in interphase (Int) or isolated midbodies (Mid) [12–14] were separated by SDS-PAGE, and the amount of dynamin and α-Tubulin present in each fraction was determined by (F) Western blot analysis with anti-Dyn2 [34] and anti-α-Tubulin antibodies, followed by (G) quantitation with densitometry. In order for dynamin to be detected in both the interphase and spindle midbody extracts at the same exposure time, the interphase extracts lane was loaded with 10-fold the amount of protein as that in the spindle midbody extracts lane. (G) Densitometric quantitation of the bands showed an approximate 30- to 50-fold enrichment of dynamin and an approximate 10- to 15-fold enrichment of α-Tubulin in spindle midbody extracts in comparison to the interphase extracts, as indicated by the graph. Quantitation was based on two separate experiments, and the error bar represents standard deviation from the mean.

sectioned, and stained with pan-dynamin antibodies (MC-63 or MC-64/MC-65) or control preimmune serum. Consistent with the immunofluorescence data, dynamin was detected along or near midbody microtubules during early telophase as the furrow ingressed (Figure 2D and data not shown) and at the electron-dense matrix of the midbody (Figure 2E). As a control, sections stained with preimmune serum did not lead to any specific labeling of the intercellular bridge (Figure 2F).

To support our morphological observations, we next tested whether an enrichment of dynamin in the intercellular bridge could be detected by Western blot analysis. CHO cell extracts were obtained from both Taxol-treated interphase cells and synchronized cells in the late stages of cytokinesis [12–14]. These extracts were subjected to SDS-PAGE, followed by Western blotting with anti-dynamin and anti-α-Tubulin antibodies (Figure 1F). The relative amounts of dynamin and α-Tubulin present in each extract were calculated by densitometric analyses of two different experiments (Figure 1G). In agreement with the morphological observations shown in Figures 1 and 2, dynamin was found to be enriched approximately 30- to 50-fold in spindle midbody extracts in comparison to interphase extracts (Figure 1G).

Dynamin Localizes to the Newly Ingressed Furrow and Midbody in *C. elegans* Embryos

The distribution and enrichment of dynamin in the midbody of mammalian cells suggested a novel function for

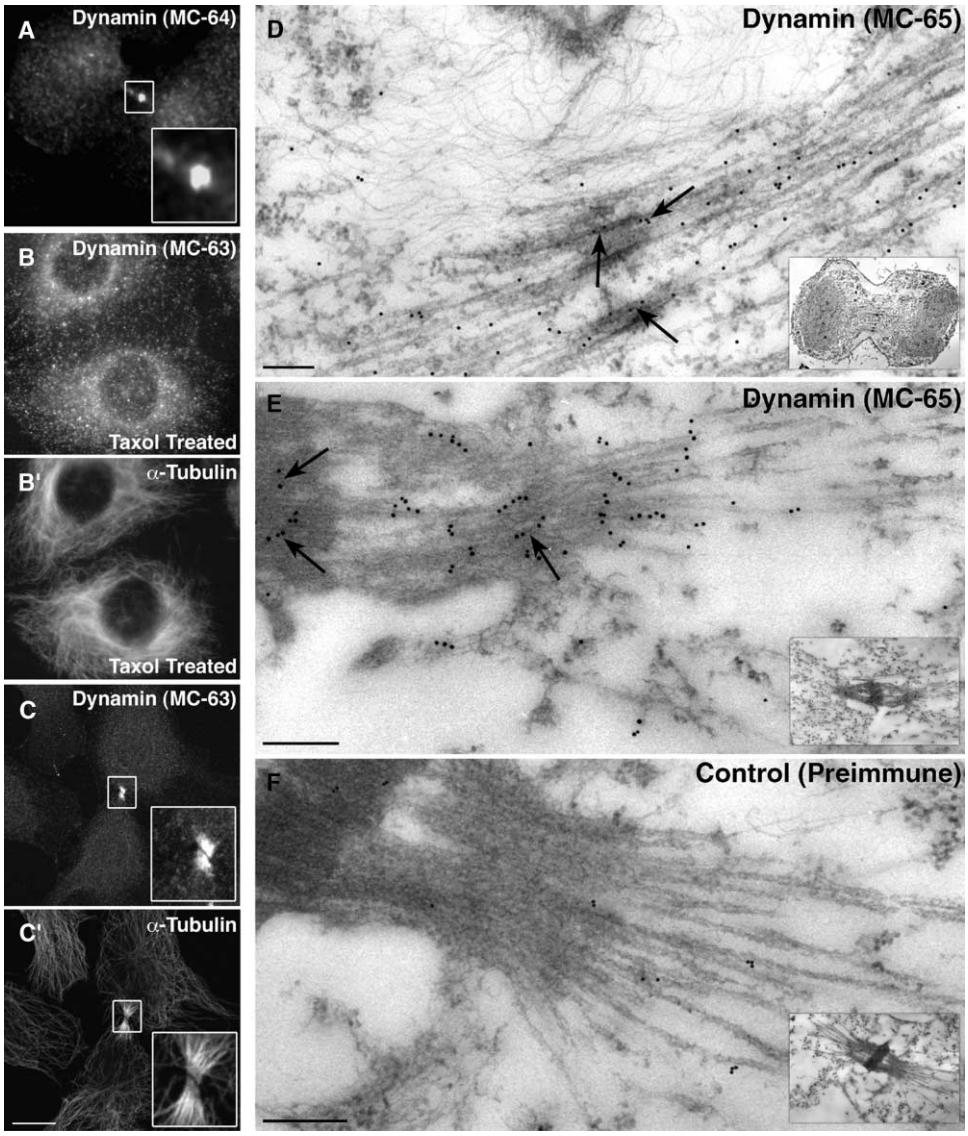

Figure 2. Immunofluorescence and Immunoelectron Microscopy Show Dynamin as a Component of the Spindle Midzone and Intercellular Bridge

To confirm the initial staining of dynamin at the intercellular bridge, a second pan-dynamin antibody to a distinct peptide, MC-64 [33], was used to stain Clone 9 cells.

(A) As shown in the inset, this dynamin antibody also recognized the region of the intercellular bridge closest to the midbody.

(B and B′) In Clone 9 cells treated with 10 μM Taxol for 1 hr, (B) dynamin did not colocalize with (B′) Taxol-induced microtubule bundles.

(C and C′) In comparison, the same pan-dynamin antibody showed an intense staining of ([C], inset) dynamin that colocalized specifically with the ([C′], inset) intercellular bridge proximal to the midbody.

(D–F) Dynamin localization at the ultrastructural level was viewed by electron microscopy in partially synchronized (D) HeLa or (E and F) L929 cells that were Triton extracted and then fixed and processed for immunoelectron microscopy [35]. Primary antibodies used were either (D and E) MC-65 [33], a pan-dynamin antibody, or, as a control, (F) preimmune serum from an MC-65 peptide-injected rabbit. Primary antibodies were recognized with either (D) Protein A-gold or (E and F) goat anti-rabbit IgG-conjugated gold particles. As seen in (D) and (E), dynamin localized to microtubule-rich regions as well as to the electron-dense matrix comprising the midbody (arrows). (F) In comparison, the control preimmune serum did not show a specific staining of the intercellular bridge or midbody. Insets show lower-magnification images of cells from which regions were magnified to show the gold particles more easily.

The scale bars in (A)–(C′) represent 10 μm, and the scale bars in (D)–(F) represent 200 nm.

dynamin in cytokinesis in mammalian cells. To test if dynamin played a role in cytokinesis in other eukaryotes that were more amenable to genetic manipulation, we used the nematode *C. elegans* [15]. In this organism, disruption of dynamin function was possible by two means: knockdown of gene expression through RNA interference (RNAi) and use of a temperature-sensitive dynamin mutant, *dyn-1(ky51)* [9]. By immunostaining early embryos with an antibody specific for the *C. elegans* dynamin homolog, we first showed that the *C. elegans* homolog to conventional dynamin localized to mitotic spindles [9]. During metaphase/early anaphase,

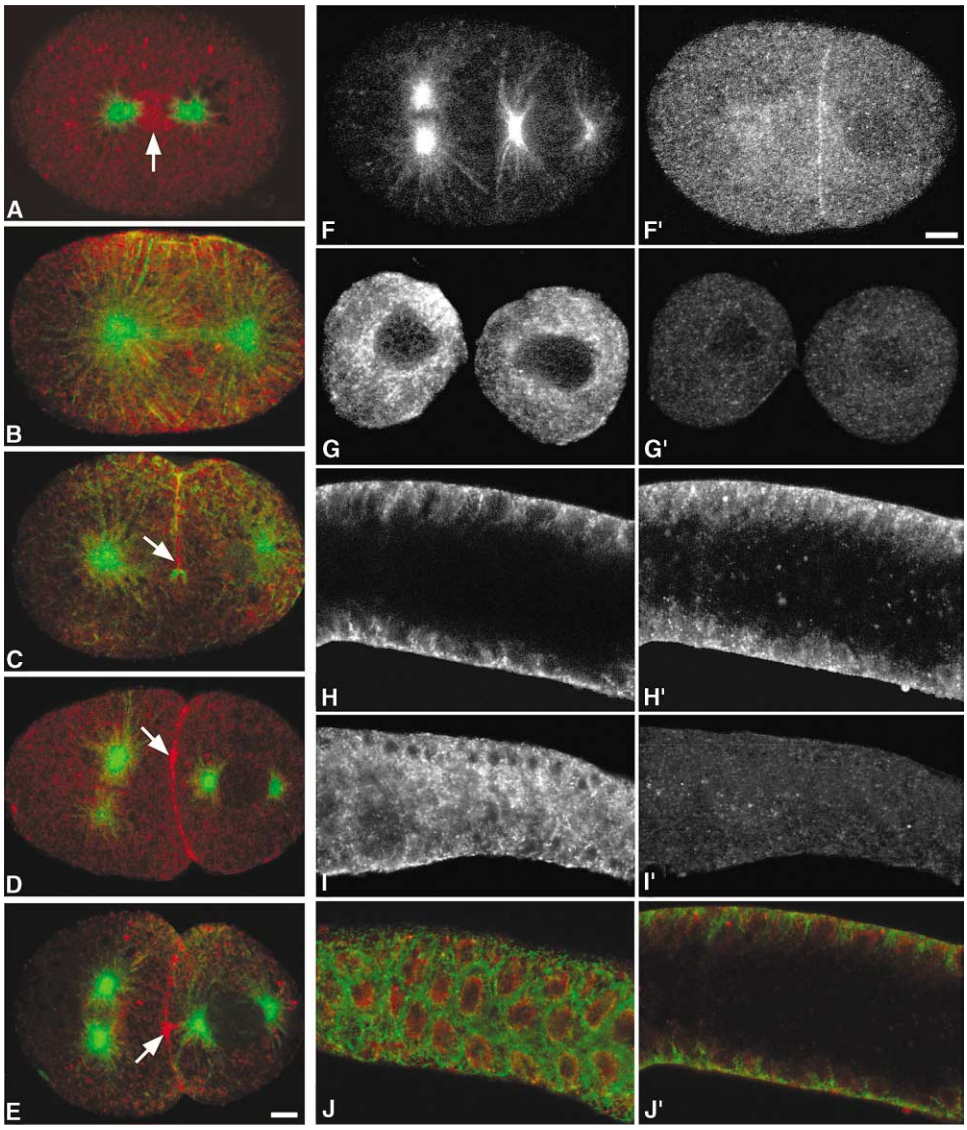

Figure 3. Dynamin Localizes to the Newly Formed Furrow Membranes and the Midbody in *C. elegans*

All embryos are arranged with anterior toward the left.

(A–E) Cells at the middle and late stages of mitosis were stained for α-Tubulin (green) and Dyn-1 (red) and were observed with a Leica confocal microscope as described previously [36]. ([A], arrow) At the metaphase-anaphase transition, dynamin was observed to localize between the asters. (B) During anaphase, dynamin appeared to localize equatorially, and a population of dynamin appeared on the midzone microtubules. ([C], arrow) During late telophase, dynamin appeared to localize only to the newly formed membrane. ([D], arrow) During early cytokinesis, dynamin localized to the newly formed membrane and along the cleavage furrow. ([E], arrow) As cytokinesis progressed, the dynamin staining became more punctate along the newly ingressed furrow, and the midbody staining was more intense.

(F–I′) To deplete *C. elegans* embryos and adults of dynamin, embryos and adults were treated with *dyn-1* RNAi and were then stained, as described previously [36], for (F–I) microtubules (as a marker for the stages of mitosis) and (F′–I′) dynamin. (G′ and I′) A marked reduction in dynamin staining as well as a (G and I) disruption of the microtubule cytoskeleton can be seen in the (G and G′) early embryo and (I and I′) adult gonad treated with *dyn-1* RNAi as compared to (F and F′ and H and H′; all gonad images are of the same focal plane) untreated control animals.

(J and J′) In the wild-type *C. elegans* gonad, dynamin resides just inside the tubulin meshwork. (J) Top and (J′) midfocal planes of merged α-Tubulin (green) and dynamin (red) staining in the gonad are shown.

The scale bars represent 5 μm.

dynamin was markedly concentrated around the metaphase plate and was also present on several large cytoplasmic vesicles (Figure 3A). Later in anaphase, dynamin became concentrated equatorially and also localized along spindle microtubules (Figure 3B) in a manner similar to the localization of dynamin along spindle microtubules in mammalian cells (Figure 1B). Further, in *C. elegans* embryos, dynamin localized to the newly formed cleavage furrow (Figures 3C–3E) and accumulated at the midbody as the embryos progressed through the

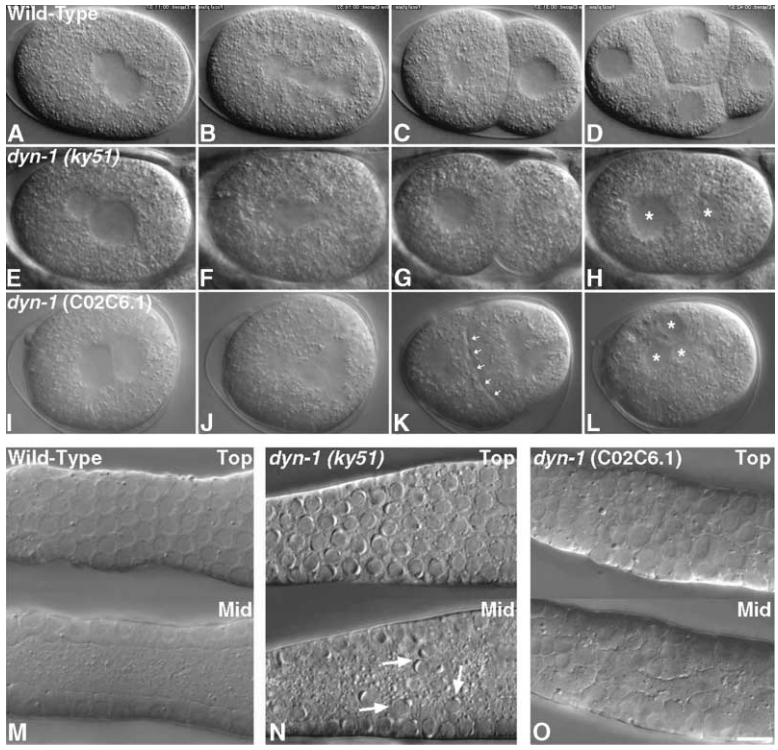

Figure 4. Dynamin Is Essential for Proper Cytokinesis and Cellularization in *C. elegans*

All embryos are arranged with anterior toward the left.

(A–L) Video microscopy was performed as described previously [11], and movies are available as Supplementary Material (available with this article online). ([A–D] and Movie 1) Images of a wild-type embryo progressing through the 1- through the 4-cell stages. The stages shown are: (A) pronuclei meet in the center, (B) the spindle sets up along the A-P axis, (C) the 2-cell embryo, (D) the 4-cell embryo. ([E–H] and Movie 2) The *dyn-1(ky51)* embryo at the restrictive temperature is not able to successfully complete cytokinesis. The stages shown are: (E) pronuclei meet in the center, (F) the spindle sets up along the A-P axis, (G) an apparent 2-cell embryo, (H) the cleavage furrow has regressed and two nuclei (asterisks) are present in the embryo. ([I–L] and Movie 3) Embryos depleted of Dyn-1 by using *dyn-1* (C02C6.1) RNAi are also unable to undergo successful cytokinesis. The stages shown are: (I) pronuclei meet in the center; (J) a tetrapolar spindle sets up (due to a previous failure in cytokinesis); (K) the furrow has apparent bubbling along the membrane (arrows), and, soon after this phenotype, the furrow regresses; (L) complete failure of cytokinesis and the embryo is multinucleate (asterisks).

(M–O) Nomarski images show top (top image) and midfocal planes (bottom image). (M) Germline nuclei are situated at the periphery of the gonad at the midfocal plane in wild-type gonads, and the rachis is devoid of germline nuclei. (N) In the *dyn-1(ky51)* mutant gonad, germline nuclei (arrows) have fallen into the rachis or common cytoplasm of the gonad. (O) As in *dyn-1(ky51)* gonads, gonads of worms treated with *dyn-1* RNAi (C02C6.1) contain germline nuclei that have fallen into the rachis, and, in addition, the nuclei appear swollen. The scale bar represents 6 μm.

early and late stages of cytokinesis (Figures 3D and 3E). Treatment of *C. elegans* embryos and gonads with *dyn-1* RNAi resulted in a depletion of dynamin staining, as observed by immunofluorescence staining (Figures 3G′ and 3I′), indicating that the dynamin gene was targeted by using RNAi and that dynamin protein expression was reduced. In addition, this observation supports the specificity of the dynamin antibody used in this study.

Cytokinetic Defects in Temperature-Sensitive *dyn-1 C. elegans* Embryos

After establishing that dynamin localizes to the midbody in *C. elegans* embryos in a manner similar to that in mammalian cells, we next tested for functional defects in cytokinesis as a result of altered dynamin function. For these studies, we used a dynamin temperature-sensitive mutant strain of *C. elegans*, *dyn-1(ky51)* [9]. In previous studies, it was noted that, after a long period at the restrictive temperature (25°C), the *dyn-1(ky51)* animals had an increase in embryonic lethality and sterility, as seen by the decrease in brood size, suggesting that dynamin may play a role in embryogenesis and incomplete cellularization of the syncytial gonad. To determine the defects leading to embryonic lethality, we observed embryos from temperature-shifted hermaphrodites by using video-microscopy [11]. At 24–36 hr postshift, consistent embryonic cytokinetic failures were observed, and maintenance of cells at 25°C for longer time periods resulted in more severe defects. In these mutant embryos, the second polar body failed to extrude and, most strikingly, a complete regression of the cleavage furrow occurred 3–4 min after an apparently normal spindle and furrow had formed. In six out of nine embryos from temperature-shifted mothers, late-stage cytokinesis defects were discovered in which the furrow was allowed to ingress completely but was then aborted (Figures 4E–4H and Movie 2 [for Movie 2, see the Supplementary Material available with this article online]).

Depletion of Dynamin with RNAi Blocks the Late Phase of Cytokinesis in *C. elegans*

To further confirm the temperature-sensitive cytokinesis defect observed in the *dyn-1(ky51) C. elegans* strain, we performed RNAi experiments to deplete embryos of dynamin. The *C. elegans* dynamin gene, *dyn-1*, corresponds to the C02C6.1 gene and is the only dynamin present in worms; thus, this gene was targeted by using RNAi as described previously [16]. Injection of dsRNA produced several cytokinetic defects at 24–36 hr after injection, and, during these times points, 100% embryonic lethality was also observed. RNAi-treated embryos ingressed fully and then regressed in 12 of 13 embryos at 22–24 hr postinjection (Figures 4I–4L and Movie 3 [for Movie 3, see the Supplementary Material available with this article online]), suggesting a role for dynamin during the late stages of cytokinesis. In these RNAi-treated embryos, an interesting furrow phenotype was observed. The ingressed furrow membrane appeared to bubble or blister just before furrow regression, as if the membrane were peeling apart or relaxing on either side

of the newly formed furrow. The lack of dynamin may have caused a relaxation of tension in the ingressed furrow membrane and ultimately a failure in cytokinesis. At longer time points after RNAi injection (30–36 hr), 14 of 19 embryos never furrowed, and 4 of 19 had late cleavage failures. Thus, dynamin could play a role during the early stages of furrow ingression as well as during the final stages of cytokinesis.

In addition to the defects in cytokinesis observed in the *dyn-1(ky51)* and RNAi-treated embryos, the *dyn-1* mutant and RNAi-injected gonads displayed syncytial germline defects that eventually led to the complete sterility of the animal. The germ cells in the *C. elegans* gonad are incompletely cellularized, like the nuclei during the syncytial divisions in the *Drosophila* embryo. This germline defect that we observe explains the underlying cause of the sterility previously observed in *dyn-1(ky51)*-shifted animals [9]. Within 24–36 hr following either treatment, gonads contained nuclei in the rachis, the common cytoplasm of the syncytial gonad (Figures 4). Thus, it appeared that furrow ingression and membrane insertion necessary for the incomplete furrows in the syncytial gonad that hold the nuclei in position were also dependent on dynamin function.

Dynamin, Cytokinesis, and Cellularization

This study provides the first demonstration for the essential role of the large GTPase dynamin in the completion of cytokinesis in animal cells. The participation of dynamin in this process appears to be evolutionarily conserved, as dynamin homologs in *Dictyostelium discoideum* [17], zebrafish [18], and plants [19–21] have been implicated in cell division. The suggestion has also been made that dynamin plays a role in *Drosophila melanogaster* cellularization [22, 23]; however, the role of dynamin in *D. melanogaster* remains largely undefined. A mechanoenzyme, such as dynamin, with lipid and protein binding domains could contribute to cytokinesis in multiple ways. First, dynamin may be involved in the fission, fusion, and remodeling of membranes at the cleavage furrow and cell plate during furrow ingression and formation of the tubular membrane network present at the cell plate. Second, dynamin could contribute to creating and maintaining tension at the cleavage furrow by tubulating furrow membranes and helping pull them inward along with the cytoskeleton as the furrow contracts. Third, dynamin could provide an essential link between the mitotic cytoskeleton and furrow membranes to facilitate membrane insertion and remodeling as well as the final separation of daughter cells. These potential mechanisms of action for dynamin are not mutually exclusive and may even overlap; thus, dynamin may contribute to cytokinesis in more ways than one.

Finally, contributions by dynamin to both membrane fusion and fission are likely to be generated through direct interactions with the mitotic cytoskeleton. Recently, the *shibire* protein, the *D. melanogaster* dynamin homolog, was identified in a biochemical screen for actin and microtubule binding proteins involved in cellularization [23]. Moreover, mammalian dynamin was originally isolated from brain as a microtubule binding protein [24] and has recently been shown to interact with the actin cytoskeleton [25–30]. As dynamin localized to microtubules of the spindle midzone and intercellular bridge, and interacts with the actin cytoskeleton as well as membranes, it is tempting to speculate that dynamin is involved in the coordination of membrane remodeling events with cytoskeletal dynamics necessary for cleavage furrow ingression and the final separation of daughter cells. Our study is consistent with the concept that plant cell plate formation and animal cell cytokinesis are analogous processes [4, 11, 31, 32] and is supportive of a conserved role for dynamin family members in these processes across a variety of species. Important questions remain to be addressed. What specific roles does dynamin play in membrane and cytoskeletal dynamics at the cleavage furrow and phragmoplast? How are dynamin localization and function regulated during mitosis and cytokinesis? What proteins and/or lipids interact with dynamin during cytokinesis? It will be interesting and important to determine the roles of dynamin in mediating and regulating cytoskeletal and membrane dynamics that permit the successful completion of cytokinesis.

Experimental Procedures

Reagents

All chemicals were purchased from Sigma unless otherwise indicated. Anti-human α-Tubulin antibody was purchased from Cedarlane and was used at a dilution of 1:1000 for immunocytochemistry. In worm embryos, the anti-α-Tubulin antibody DM1A from ICN, Pharmaceuticals was used. The anti-dynamin antibodies used, MC-63, MC-64/MC-65, and Dyn2, have been previously characterized [33, 34] and were used at 5 μg/ml for immunocytochemistry, 15 μg/ml for immunoelectron microscopy, and 0.5 μg/ml for Western blotting. The Dyn-1 antibody used to recognize the *C. elegans* Dyn-1 protein has been described previously [9]. Secondary antibodies used for immunocytochemistry were Texas red-conjugated goat anti-mouse and FITC- or Alexa 488-conjugated goat anti-rabbit, all from Molecular Probes. DAPI staining was used as a marker for DNA (a gift of Dr. Greg Gores, Rochester, MN). Secondary antibodies used for Western blotting were HRP-conjugated goat anti-mouse and HRP-conjugated goat anti-rabbit, both from Biosource. Digital images were rendered with Adobe PhotoShop 6.0 software (Adobe Photosystems).

C. elegans Strains and *dyn-1* RNAi

The wild-type N2 strain was a kind gift from the *C. elegans* Stock Center. The *dyn-1* temperature-sensitive mutant *dyn-1(ky51)* was a kind gift of Alexander van der Bliek. The *dyn-1(ky51)* worms were shifted to 25°C for 24–36 hr during experiments.

Double-stranded RNA was synthesized with double T7 primers against the C02C6.1 gene by using the Ambion Megascript T7 kit (Ambion) as stated previously [11]. The dsRNA was injected into N2 hermaphrodite gonads, and embryos were cut out of mothers and mounted as stated in [11] and were observed in the 24–36 hr timeframe. Dissected gonads were also observed for defects.

Supplementary Material

Supplementary Material including movies of wild-type, the *dyn-1 ts* mutant, and *dyn-1* RNAi-treated *C. elegans* embryos undergoing cytokinesis is available at http://images.cellpress.com/supmat/supmatin.htm.

Acknowledgments

The authors thank Alexander van der Bliek for the *dyn-1(ky51)* worm strain and the Dyn-1 antibody. We also thank John White, Rebecca Heald, Kirsten Hagstrom, Diana Chu, Ed Ralston, Annette Chan, and the Meyer, Heald, and McNiven labs for support, discussion, and reading of the manuscript. A.R.S. is supported by National Institutes

of Health (NIH) grant F32 GM64159-01. M.A.M. is supported by NIH grant DK 44650-11. B.J.M. is an investigator of the Howard Hughes Medical Institute.

Received: August 5, 2002
Revised: September 16, 2002
Accepted: October 4, 2002
Published: December 23, 2002

References

1. Glotzer, M. (2001). Animal cell cytokinesis. Annu. Rev. Cell Dev. Biol. *17*, 351–386.
2. Straight, A.F., and Field, C.M. (2000). Microtubules, membranes and cytokinesis. Curr. Biol. *10*, R760–R770.
3. Robinson, D.N., and Spudich, J.A. (2000). Towards a molecular understanding of cytokinesis. Trends Cell Biol. *10*, 228–237.
4. Bowerman, B., and Severson, A.F. (1999). Cell division: plant-like properties of animal cell cytokinesis. Curr. Biol. *9*, R658–R660.
5. O'Halloran, T.J. (2000). Membrane traffic and cytokinesis. Traffic *1*, 921–926.
6. Finger, F.P., and White, J.G. (2002). Fusion and fission: membrane trafficking in animal cytokinesis. Cell *108*, 727–730.
7. McNiven, M.A., Cao, H., Pitts, K.R., and Yoon, Y. (2000). The dynamin family of mechanoenzymes: pinching in new places. Trends Biochem. Sci. *25*, 115–120.
8. Hinshaw, J.E. (2000). Dynamin and its role in membrane fission. Annu. Rev. Cell Dev. Biol. *16*, 483–519.
9. Clark, S.G., Shurland, D.L., Meyerowitz, E.M., Bargmann, C.I., and van der Bliek, A.M. (1997). A dynamin GTPase mutation causes a rapid and reversible temperature-inducible locomotion defect in *C. elegans*. Proc. Natl. Acad. Sci. USA *94*, 10438–10443.
10. Shuster, C.B., and Burgess, D.R. (2002). Targeted new membrane addition in the cleavage furrow is a late, separate event in cytokinesis. Proc. Natl. Acad. Sci. USA *99*, 3633–3638.
11. Skop, A.R., Bergmann, D., Mohler, W.A., and White, J.G. (2001). Completion of cytokinesis in *C. elegans* requires a brefeldin A-sensitive membrane accumulation at the cleavage furrow apex. Curr. Biol. *11*, 735–746.
12. Mullins, J.M., and McIntosh, J.R. (1982). Isolation and initial characterization of the mammalian midbody. J. Cell Biol. *94*, 654–661.
13. Kuriyama, R., Keryer, G., and Borisy, G.G. (1984). The mitotic spindle of Chinese hamster ovary cells isolated in taxol-containing medium. J. Cell Sci. *66*, 265–275.
14. Kuriyama, R., and Ensrud, K. (1999). Obtaining antibodies to spindle components. Methods Cell Biol. *61*, 233–244.
15. Brenner, S. (1974). The genetics of *Caenorhabditis elegans*. Genetics *77*, 71–94.
16. Fire, A., Xu, S., Montgomery, M.K., Kostas, S.A., Driver, S.E., and Mello, C.C. (1998). Potent and specific genetic interference by double-stranded RNA in *Caenorhabditis elegans*. Nature *391*, 806–811.
17. Wienke, D.C., Knetsch, M.L.W., Neuhaus, E.M., Reedy, M.C., and Manstein, D.J. (1999). Disruption of a dynamin homologue affects endocytosis, organelle morphology, and cytokinesis in *Dictyostelium discoideum*. Mol. Biol. Cell *10*, 225–243.
18. Feng, B., Schwarz, H., and Jesuthasan, S. (2002). Furrow-specific endocytosis during cytokinesis of zebrafish blastomeres. Exp. Cell Res. *279*, 14–20.
19. Otegui, M.S., Mastronarde, D.N., Kang, B.-H., Bednarek, S.Y., and Staehelin, L.A. (2001). Three-dimensional analysis of syncytial-type cell plates during endosperm cellularization visualized by high resolution electron tomography. Plant Cell *13*, 2033–2051.
20. Gu, X., and Verma, D.P. (1996). Phragmoplastin, a dynamin-like protein associated with cell plate formation in plants. EMBO J. *15*, 695–704.
21. Lauber, M.H., Waizenegger, I., Steinmann, T., Schwarz, H., Mayer, U., Hwang, I., Lukowitz, W., and Jürgens, G. (1997). The *Arabidopsis* KNOLLE protein is a cytokinesis-specific syntaxin. J. Cell Biol. *139*, 1485–1493.
22. Swanson, M.M., and Poodry, C.A. (1981). The *shibire*^{ts} mutant of *Drosophila*: a probe for the study of embryonic development. Dev. Biol. *84*, 465–470.
23. Sisson, J.C., Field, C., Ventura, R., Royou, A., and Sullivan, W. (2000). Lava lamp, a novel peripheral golgi protein, is required for *Drosophila melanogaster* cellularization. J. Cell Biol. *151*, 905–918.
24. Shpetner, H.S., and Vallee, R.B. (1989). Identification of dynamin, a novel mechanochemical enzyme that mediates interactions between microtubules. Cell *59*, 421–432.
25. Ochoa, G.-C., Slepnev, V.I., Neff, L., Ringstad, N., Takei, K., Daniell, L., Cao, H., McNiven, M.A., Baron, R., and De Camilli, P. (2000). A functional link between dynamin and the actin cytoskeleton at podosomes. J. Cell Biol. *150*, 377–389.
26. Lee, E., and De Camilli, P. (2002). Dynamin at actin tails. Proc. Natl. Acad. Sci. USA *99*, 161–166.
27. Orth, J.D., Krueger, E.W., Cao, H., and McNiven, M.A. (2002). The large GTPase dynamin regulates actin comet formation and movement in living cells. Proc. Natl. Acad. Sci. USA *99*, 167–172.
28. McNiven, M.A., Kim, L., Krueger, E.W., Orth, J.D., Cao, H., and Wong, T.W. (2000). Interactions between dynamin and the actin binding protein cortactin modulate cell shape. J. Cell Biol. *151*, 187–198.
29. Kessels, M.M., Engqvist-Goldstein, A.E., Drubin, D.G., and Qualmann, B. (2001). Mammalian Abp1, a signal-responsive F-actin-binding protein, links the actin cytoskeleton to endocytosis via the GTPase dynamin. J. Cell Biol. *153*, 351–366.
30. Witke, W., Podtelejnikov, A.V., Di Nardo, A., Sutherland, J.D., Gurniak, C.B., Dott, C., and Mann, M. (1998). In mouse brain profilin I and profilin II associate with regulators of the endocytic pathway and actin assembly. EMBO J. *17*, 967–976.
31. Hales, K.G., Bi, E., Wu, J.-Q., Adam, J.C., Yu, I.-C., and Pringle, J.R. (1999). Cytokinesis: an emerging unified theory for eukaryotes? Curr. Opin. Cell Biol. *11*, 717–725.
32. Field, C., Li, R., and Oegema, K. (1999). Cytokinesis in eukaryotes: a mechanistic comparison. Curr. Opin. Cell Biol. *11*, 68–80.
33. Henley, J.R., and McNiven, M.A. (1996). Association of a dynamin-like protein with the Golgi apparatus in mammalian cells. J. Cell Biol. *133*, 761–775.
34. Henley, J.R., Krueger, E.W., Oswald, B.J., and McNiven, M.A. (1998). Dynamin-mediated internalization of caveolae. J. Cell Biol. *141*, 85–99.
35. Euteneuer, U., Gräf, R., Kube-Granderath, E., and Schliwa, M. (1998). *Dictyostelium* γ-tubulin: molecular characterization and ultrastructural localization. J. Cell Sci. *111*, 405–412.
36. Skop, A.R., and White, J.G. (1998). The dynactin complex is required for cleavage plane specification in early *Caenorhabditis elegans* embryos. Curr. Biol. *8*, 1110–1116.